

## LAMINAR NATURAL CONVECTION FROM A VERTICAL PLATE WITH VARIATIONS IN SURFACE HEAT FLUX

S. Lee, Graduate Research Assistant and M. M. Yovanovich, Professor  
Microelectronics Heat Transfer Laboratory  
Department of Mechanical Engineering  
University of Waterloo  
Waterloo, Ontario, Canada

### ABSTRACT

Two-dimensional natural convection heat transfer from a vertical plate is studied for a family of non-similar surface heat flux variations. The investigation resulted in an approximate but simple analytical method that predicts the local temperature and velocity distributions for laminar boundary layer flow over a wide range of Prandtl numbers. A derivation is detailed, and a number of illustrative results are presented. The downstream variations of wall temperature and maximum velocity level are compared with existing numerical data, which was obtained for a case in air with a uniform surface heat flux element mounted flush on a vertical adiabatic surface. The agreement is good, and the qualitative characteristics of the new results are consistent with those described in the numerical study. The method also adequately reproduces the results that were predicted by using similarity methods for the case with a line thermal source on an adiabatic surface.

### NOMENCLATURE

$a, A$	constants in Eq. (28)
$\tilde{a}, \tilde{A}$	constants in Eq. (4)
$\tilde{b}, \tilde{B}$	constants in Eq. (4)
$\tilde{C}$	constant, $\tilde{C} = (\sqrt{\text{Pr}} \tilde{C}_u/4)^{2/3}$ or $\tilde{C} = \text{Pr}/(4\tilde{C}_\eta^2)$
$C_u, C_\eta$	constants used in Eqs. (29) and (30)
$\tilde{C}_u, \tilde{C}_\eta$	constants in Eqs. (11) and (12)
$\text{erfc } z$	complementary error function, $\frac{2}{\sqrt{\pi}} \int_z^\infty e^{-\tau^2} d\tau$
$f_T, f_u$	functions defined by Eqs. (20) and (21)
$g$	gravitational acceleration
$h_e, h_m$	functions defined by Eqs. (A.10) and (A.9)
$\chi_e, \chi_m$	functions defined by Eqs. (A.6) and (A.5)
$i^{\tilde{n}} \text{erfc } z$	complementary error function integrated $\tilde{n}$ -times, $\int_z^\infty i^{\tilde{n}-1} \text{erfc } \tau d\tau$ , $i^1 \text{erfc } z = \text{ierfc } z$ , $i^0 \text{erfc } z = \text{erfc } z$
$k$	thermal conductivity of fluid

$\tilde{m}, \mathcal{M}$	constants in Eq. (7)
$n$	constant defined by Eq. (31) or Eq. (34)
$\tilde{n}, \mathcal{N}$	constants in Eq. (7)
$p$	square root of Prandtl number, $\sqrt{\text{Pr}}$
$q$	local heat flux
$q^*$	non-dimensionalized local heat flux, $q/q_{w0}$
$q_e^*, q_m^*$	parameters defined by Eqs. (A.8) and (A.7)
$t$	<i>pseudo-time</i> defined in $t-y$ plane
$t_0$	<i>pseudo-time</i> when $x = x_0$
$T$	temperature excess over ambient fluid temperature
$T^*$	non-dimensionalized temperature excess, $T/T_{w0}$
$u$	local velocity parallel to plate, in $x$ -direction
$u_c$	characteristic $u$ -velocity across the boundary layer
$v$	local velocity normal to plate, in $y$ -direction
$x$	vertical coordinate measured from leading edge
$x_0$	value of $x$ at which functional discontinuity of wall temperature occurs, see Eq. (4)
$y$	horizontal coordinate measured from plate surface

### Greek Symbols

$\alpha$	thermal diffusivity of fluid, $k/(\rho c_p)$
$\beta$	thermal expansion coefficient, $-(\partial\rho/\partial T)_P/\rho$
$\gamma$	parameter, $\eta_0/\eta_1$ or $\sqrt{(1-1/\xi)\tilde{\psi}/\tilde{\phi}}$
$\Gamma(z)$	Gamma function, $\int_0^\infty t^{z-1} e^{-t} dt$
$\eta_0$	variable, $y/\sqrt{4\alpha t}$ in $t-y$ plane, or $\tilde{C}_\eta/\sqrt{\tilde{\phi}} \cdot \text{Gr}_x^{*1/5} \cdot y/x$ in $x-y$ plane
$\eta_1$	variable, $y/\sqrt{4\alpha(t-t_0)}$ in $t-y$ plane, or $\tilde{C}_\eta/\sqrt{(1-1/\xi)\tilde{\psi}} \cdot \text{Gr}_x^{*1/5} \cdot y/x$ in $x-y$ plane
$\Lambda(\tilde{n})$	parameter, $\Lambda(\tilde{n}) = 1/i^{\tilde{n}} \text{erfc } 0 = 2^{\tilde{n}} \Gamma(\tilde{n}/2 + 1)$
$\nu$	kinematic viscosity, $\mu/\rho$
$\xi$	non-dimensionalized $x$ -coordinate, $x/x_0$
$\tilde{\phi}, \tilde{\psi}$	modifying functions defined in Eqs. (16) and (17), $\tilde{\phi} = 1$ when $x \leq x_0$

## Subscripts

$w0$	wall conditions for $x \leq x_0$
$w1$	wall conditions for $x > x_0$

## Dimensionless Groups

$Gr_z^*$	modified Grashof number, $g\beta q_{w0}x^4/k\nu^2$
$Nu_z$	local Nusselt number, $q_{w0}x/T_{w0}k$
$Pr$	Prandtl number, $\nu/\alpha$
$Ra_z^*$	modified Rayleigh number, $Gr_z^* \cdot Pr$

## INTRODUCTION

The study of natural convection heat transfer from a vertical plate with a number of finite size heat sources has attracted a great deal of interest over the past years. It has direct applications to thermal design of microelectronic circuit boards, and other energy dissipating equipment under limiting situations. Interests are focussed mainly on determining the magnitude and location of the local maximum surface temperature, and on understanding the downstream effects of the thermal plume produced by a heated element.

Numerous investigators, using various methods and techniques, have worked on cases of a step change in uniform wall temperature (Schetz and Eichhorn, 1964, Hayday et al., 1967, Smith, 1970, Kelleher, 1971, Kao, 1975, Sokovishin and Érman, 1982, Lee and Yovanovich, 1987). This thermal condition is non-similar and renders mathematical singularities to the boundary layer equations at the leading edge of the plate and at the point of discontinuity. Thus, the resulting surface heat flux becomes unbounded at these locations.

Conjugate problems, which concurrently account for the effects of heat conduction through the plate and heat convection in the surrounding fluids, have been studied numerically with experimental corroboration by Zinnes (1970), Kishinami and Seki (1983), and Kishinami et al. (1987).

The plate with prescribed heat flux variations has not received much attention to date, despite the fact that it often simulates realistic situations better than the plate with prescribed temperature variations. Only recently, Jaluria (1982, 1985), using numerical methods, solved the two-dimensional boundary layer equations, and the full elliptic equations for problems with finite size uniform heat flux elements distributed over an adiabatic surface. The solutions of the full elliptic equations reveal non-boundary layer effects in the temperature and velocity fields.

In this paper, the two-dimensional natural convection heat transfer from a vertical plate with a family of non-similar surface heat flux variations is considered. The plate is semi-infinite and suspended in a quiescent fluid which is maintained at uniform temperature. This study deals with boundary layer type problems and is an extension of an approximate method recently developed by the present authors in an earlier study (Lee and Yovanovich, 1987).

A similar approximate approach has been adopted as before, and the analysis is presented in such a manner that offers a direct comparison with that of the earlier study. The method utilizes a linearization technique, formally called the

Rayleigh transformation, with the von Kármán-Pohlhausen integral method, and results in a simple analytical model. The model predicts the local temperature and velocity distributions for the laminar boundary layer flow over a wide range of Prandtl numbers. Comparisons are made with the aforementioned numerical data of Jaluria (1985), for the case in air with a step change in uniform surface heat flux. Also, comparisons are made with the results obtained by using the similarity methods for the case with a line thermal source on an adiabatic surface (Jaluria and Gebhart, 1977). It is shown that the downstream variations of wall temperature and maximum velocity level are in good agreement. A separate study (Lee, 1988), which further extends the present model, shows a possible application of this method to problems with general heat flux variations at the wall.

## ANALYSIS

**Governing Equations.** The natural convection problem under consideration deals with a vertical flat plate of large transverse dimension with a surface heat flux variation prescribed along the wall. The plate is located in an ambient fluid which is maintained at uniform temperature. The conservation of mass, momentum and energy for two-dimensional, steady-state, laminar boundary layer flow yields the usual set of governing differential equations expressed as

$$\frac{\partial u}{\partial x} + \frac{\partial v}{\partial y} = 0 \quad (1)$$

$$u \frac{\partial u}{\partial x} + v \frac{\partial u}{\partial y} = \nu \frac{\partial^2 u}{\partial y^2} + g\beta T \quad (2)$$

$$u \frac{\partial T}{\partial x} + v \frac{\partial T}{\partial y} = \alpha \frac{\partial^2 T}{\partial y^2} \quad (3)$$

where  $x$  and  $y$  are coordinates parallel and normal to the plate, respectively,  $u$  and  $v$  are corresponding components of the velocity, and  $T$  is the local temperature excess over the ambient fluid temperature. These boundary layer equations assume constant fluid properties except density variation which is needed in the derivation of the buoyant term, the driving force of the flow. The dynamic pressure work and viscous dissipation terms with other minor effects have been neglected in the above equations. The boundary conditions are

$$\begin{aligned} \text{at } y = 0, \quad u = v = 0, \\ -k \frac{\partial T}{\partial y} = q_{w0} = Ax^{\bar{a}} \quad \text{for } x \leq x_0 \\ -k \frac{\partial T}{\partial y} = q_{w1} = Ax^{\bar{a}} + B(x - x_0)^{\bar{b}} \quad \text{for } x > x_0 \end{aligned} \quad (4)$$

$$\begin{aligned} \text{as } y \rightarrow \infty, \quad u \rightarrow 0, \quad T \rightarrow 0 \\ \text{at } x = 0, \quad u = T = 0 \end{aligned}$$

where  $\bar{a}$ ,  $\bar{b}$ ,  $A$  and  $B$  are constants.

Since the boundary layer approximations assume no diffusion along the flow direction, the solution to the above set of equations becomes less valid in the immediate vicinity of the

leading edge, at  $x = 0$ , and the location of functional change, at  $x = x_0$ . The quantitative discrepancy introduced by the approximations has been examined by Jaluria (1985), who solved a full set of two-dimensional elliptic equations by employing finite difference methods. Consider a plate generating heat with negligible lateral thermal conduction. The plate dissipates energy directly into the fluid, and the surface heat flux variation thus coincides with the internal heat generation of the plate, as such  $q_{w0} > 0$  and  $q_{w1} \geq 0$ . The present analysis also allows  $q_{w1}$  to become negative, meaning the fluid is heating the plate, provided that the temperature excess at any point within the fluid is maintained positive.

**Pseudo-Transient Equations.** The set of equations, Eqs. (1-3), with the foregoing boundary conditions represents an extremely complicated mathematical problem. The momentum and energy equations are mutually coupled and are non-linear. Similarity solutions exist for  $x \leq x_0$ , but not for  $x > x_0$ .

An approximate method which transforms the  $x$ -coordinate into a *pseudo-transient* coordinate  $t$  is introduced. A relationship, called the Rayleigh transformation, between  $x$  and  $t$  is established as  $x = u_c \times t$ , where  $u_c$  represents a characteristic streamwise velocity across the boundary layer. Since  $u_c$  is dependent only on  $x$  in space, a fixed downstream location  $x$  corresponds to a fixed *pseudo-time*  $t$  over the boundary layer, and the original  $x - y$  plane is transformed into the  $t - y$  plane. An assumption is made such that diffusion is dominant across the boundary layer in the  $y$ -direction at any given time. This implies that the temperature and velocity profiles would take the form of transient conduction heat transfer into a half space. Subsequently, the convective derivatives in the  $x - y$  plane, shown on the left hand side of Eqs. (2) and (3), are replaced by the transient derivatives, resulting in the following pseudo-transient equations:

$$\frac{\partial u}{\partial t} = \nu \frac{\partial^2 u}{\partial y^2} + g\beta T \quad (5)$$

$$\frac{\partial T}{\partial t} = \alpha \frac{\partial^2 T}{\partial y^2} \quad (6)$$

The associated boundary conditions that are compatible with those in the  $x - y$  plane are

$$\begin{aligned} \text{at } y = 0, \quad u &= 0, \\ -k \frac{\partial T}{\partial y} &= q_{w0} = Nt^{\bar{n}/2} \quad \text{for } t \leq t_0 \\ -k \frac{\partial T}{\partial y} &= q_{w1} = Mt^{\bar{n}/2} + M(t - t_0)^{\bar{m}/2} \quad \text{for } t > t_0 \end{aligned} \quad (7)$$

$$\begin{aligned} \text{as } y \rightarrow \infty, \quad u &\rightarrow 0, \quad T \rightarrow 0 \\ \text{at } t = 0, \quad u &= T = 0 \end{aligned}$$

where  $\bar{n}$ ,  $\bar{m}$ ,  $N$  and  $M$  are constants,  $t$  is the transformed pseudo-time, and  $t_0$  is the corresponding time of the discontinuity at  $x_0$ .

The velocity normal to the wall does not appear in these equations. Consequently, the continuity equation, Eq. (1), becomes irrelevant in the  $t - y$  plane. A qualitative discussion

regarding this omission of the  $v$ -velocity has been briefly carried out by Lee and Yovanovich (1987). The most notable features that are different in these transformed equations from the steady-state equations are the linearity of the dependent variables  $u$  and  $T$ , and the unilateral decoupling of the temperature field from the velocity field.

The solutions to the above transient equations with the specified boundary conditions are obtained by means of either Laplace transforms (Schetz and Eichhorn, 1962, Menold and Yang, 1962), or similarity methods (Lee, 1988). The resulting solutions for  $t > t_0$  are

$$T = \frac{2\sqrt{\alpha}}{k} [q_{w0} t^{1/2} \Lambda(\bar{n}) i^{\bar{n}+1} \text{erfc } \eta_0 + (q_{w1} - q_{w0})(t - t_0)^{1/2} \Lambda(\bar{m}) i^{\bar{m}+1} \text{erfc } \eta_1] \quad (8)$$

$$u = \begin{cases} \frac{4\sqrt{\alpha}g\beta}{k} [q_{w0} t^{3/2} \Lambda(\bar{n}) \eta_0 i^{\bar{n}+2} \text{erfc } \eta_0 + (q_{w1} - q_{w0})(t - t_0)^{3/2} \Lambda(\bar{m}) \eta_1 i^{\bar{m}+2} \text{erfc } \eta_1] & \text{for Pr} = 1 \\ \frac{4\sqrt{\alpha}g\beta}{k} \frac{2}{1 - \text{Pr}} \left[ q_{w0} t^{3/2} \Lambda(\bar{n}) (i^{\bar{n}+3} \text{erfc } \eta_0 - i^{\bar{n}+3} \text{erfc } \frac{\eta_0}{\sqrt{\text{Pr}}}) + (q_{w1} - q_{w0})(t - t_0)^{3/2} \right. \\ \left. \times \Lambda(\bar{m}) (i^{\bar{m}+3} \text{erfc } \eta_1 - i^{\bar{m}+3} \text{erfc } \frac{\eta_1}{\sqrt{\text{Pr}}}) \right] & \text{for Pr} \neq 1 \end{cases} \quad (9)$$

where  $\bar{n}$  and  $\bar{m}$  are integers that are greater than or equal to  $-2$ ,  $\eta_0 = y/\sqrt{4\alpha t}$ ,  $\eta_1 = y/\sqrt{4\alpha(t - t_0)}$ , and  $\Lambda(\bar{n}) = 2^{\bar{n}} \Gamma(\frac{\bar{n}}{2} + 1)$ . The above solutions were developed based on the method of superposition, and the first terms represent the solutions for  $t \leq t_0$ .

Note that  $\bar{n} = \bar{m} = 0$  denotes uniform  $q_{w0}$  and  $q_{w1}$ , and  $\bar{n} = \bar{m} = -1$  is the condition for uniform  $T_{w0}$  and  $T_{w1}$  in the  $t - y$  plane. However, it will be observed that the latter condition does not correspond to uniform  $T_{w1}$  in the  $x - y$  plane, for which the superposition is not allowed. This is discussed further after the presentation of the reverse transformations of the pseudo-time onto the spacial coordinates.

Now, the problem is reduced to finding a proper characteristic velocity or velocities,  $u_c(x)$ , over the boundary layer, and the values of  $\bar{n}$  and  $\bar{m}$ . Determination of  $u_c(x)$  defines the transformation functions that will, in turn, convert the  $t - y$  plane carrying the above solutions back to the  $x - y$  plane.

**$t - x$  Transformations for  $x \leq x_0$ .** The parameters from the steady-state solutions for the given surface heat flux variations, and those appearing in the above pseudo-transient solutions are compared as follows:

$$\text{Surface Heat Flux} \quad ; \quad Ax^{\bar{a}} = Nt^{\bar{n}/2} \quad (10)$$

$$\text{Reference Velocity Group} \quad ; \quad \tilde{C}_u \frac{\nu}{x} \text{Gr}_x^{2/5} = \frac{4\sqrt{\alpha}g\beta}{k} q_{w0} t^{3/2} \quad (11)$$

$$\text{Similarity Variable} \quad ; \quad \tilde{C}_\eta \text{Gr}_x^{1/5} \frac{y}{x} = \frac{y}{2\sqrt{\alpha t}} \quad (12)$$

where  $\tilde{C}_u$  and  $\tilde{C}_\eta$  are dimensionless proportionality constants, functions only of the exponent  $\bar{a}$  and the Prandtl number. The parameters shown on the left hand side of the above comparisons are from the similarity analysis of Sparrow and Gregg

(1956). Although they have reported the similarity transformations for the case of uniform surface heat flux, it can be verified that the same parameters are valid for the present boundary conditions of the power form at  $x \leq x_0$ . This verification will become apparent after the discussions in the following sections.

A manipulation of either Eq. (11) or Eq. (12) upon substitution of Eq. (10) for  $q_{w0}$  yields

$$\bar{n} = \frac{5\bar{a}}{1-\bar{a}} \quad (13)$$

By rearranging Eqs. (11) and (12) for  $t$ , we find, respectively,

$$t = \left( \frac{\sqrt{\text{Pr}} \bar{C}_u}{4} \right)^{2/3} \frac{x}{\frac{v}{z} \text{Gr}_z^{2/5}} \quad (14)$$

$$t = \frac{\text{Pr}}{4\bar{C}_\eta^2} \frac{x}{\frac{v}{z} \text{Gr}_z^{2/5}} \quad (15)$$

Both Eqs. (14) and (15) express an identical functional form for the characteristic velocity such that  $u_c = v/x \cdot \text{Gr}_z^{2/5} / \bar{C}$ , where  $\bar{C} = (\sqrt{\text{Pr}} \bar{C}_u / 4)^{2/3}$  or  $\bar{C} = \text{Pr} / (4\bar{C}_\eta^2)$ . The former equation defines the time anticipated in the reference velocity group and the latter defines the time anticipated in the similarity variable. The values of the constants  $\bar{C}_u$  and  $\bar{C}_\eta$  are determined by employing the von Kármán-Pohlhausen integral method, and the derivation is provided in the appendix.

$t-x$  Transformations for  $x > x_0$ . Superposition of the transformation functions is invalid, due to the non-linearity of the problem. The  $t-x$  transformations are sought by adjusting the characteristic streamwise velocity as follows:

$$t = \frac{x}{u_c} = \bar{C} \bar{\phi} \frac{x}{\frac{v}{z} \text{Gr}_z^{2/5}} \quad (16)$$

$$t - t_0 = \frac{x - x_0}{u_c} = \bar{C} \bar{\psi} \frac{x - x_0}{\frac{v}{z} \text{Gr}_z^{2/5}} \quad (17)$$

where  $\bar{C}$  denotes, as previously defined, two different coefficients. The function  $\bar{\phi}$  in Eq. (16) modifies the characteristic velocity that would have been attained at the location of interest if the thermal condition at the wall were maintained at  $q_{w0}$ . The other function,  $\bar{\psi}$  in Eq. (17), represents the ratio of the existing characteristic velocity over a new one that characterizes the flow velocity in the secondary boundary layer initiated at  $x = x_0$ .

The modifying functions,  $\bar{\phi}$  and  $\bar{\psi}$ , are dimensionless and dependent on the exponents  $\bar{a}$  and  $\bar{b}$ ,  $\text{Pr}$ ,  $q_{w1}^*$  and  $\xi$ , where  $q_{w1}^* = q_{w1}/q_{w0}$  and  $\xi = x/x_0$ . The von Kármán-Pohlhausen integral method is again employed in evaluating  $\bar{\phi}$  and  $\bar{\psi}$ . The derivation is described in the appendix for cases where  $\bar{a} = \bar{b}$ .

An interesting and important observation can be drawn from Eq. (17). Though  $t_0$ , the corresponding pseudo-time at fixed  $x_0$ , is constant in the  $t-y$  plane, it is no longer possible to isolate the fixed  $t_0$  in the  $x-y$  plane. This makes the term  $t-t_0$  a unique variable, and, for the same reason, the time  $t$  in Eq. (17) is not the same  $t$  as in Eq. (16). The fact that there are two distinct time-spacial transformations, and the existing characteristic velocity had to be modified by  $\bar{\phi}$ , are

all parts of conditions that are required if the non-linearity of the problem was to be restored through the transformation functions for  $x > x_0$ .

Recognizing that the present solutions must approach another set of similarity solutions written in terms of  $q_{w1}$  at large  $x$ , when  $\bar{b} = \bar{a}$ , it is suggested to use the same relationship, given by Eq. (13), between  $\bar{m}$  and  $\bar{b}$  in place of  $\bar{n}$  and  $\bar{a}$ . Also, note that the coefficient  $\bar{C}$  in Eq. (17) is dependent on  $\bar{b}$ , whereas that in Eq. (16) is dependent on  $\bar{a}$ . Hence, if  $\bar{b} \neq \bar{a}$ ,  $\bar{C}$  in Eq. (17) has to be evaluated separately from the appendix with the corresponding values of the exponents.

## RESULTS AND DISCUSSION

Upon substitution of the forefound transformations, Eqs. (16) and (17), into the pseudo-transient solutions given by Eqs. (8) and (9), a set of approximate solutions in the  $x-y$  plane is obtained. For simplicity, only the cases of  $\bar{a} = \bar{b}$  are considered in this section. The resulting set of non-dimensionalized solutions for  $x > x_0$  may be expressed as

$$\frac{T}{q_{w0}x/k\text{Gr}_z^{1/5}} = \frac{\sqrt{\bar{\phi}}}{\bar{C}_\eta} \Lambda(\bar{n}) [f_T(\eta_0) + (q_{w1}^* - 1)\gamma f_T(\eta_1)] \quad (18)$$

$$\frac{u}{\frac{v}{z} \text{Gr}_z^{2/5}} = \bar{C}_u \bar{\phi}^{3/2} \Lambda(\bar{n}) [f_u(\eta_0) + (q_{w1}^* - 1)\gamma^3 f_u(\eta_1)] \quad (19)$$

where

$$f_T(\eta) = i^{\bar{a}+1} \text{erfc } \eta \quad (20)$$

$$f_u(\eta) = \begin{cases} \eta i^{\bar{a}+2} \text{erfc } \eta & \text{for } \text{Pr} = 1 \\ \frac{2}{1-\text{Pr}} (i^{\bar{a}+3} \text{erfc } \eta - i^{\bar{a}+3} \text{erfc } \frac{\eta}{\sqrt{\text{Pr}}}) & \text{for } \text{Pr} \neq 1 \end{cases} \quad (21)$$

$\eta_0 = \bar{C}_\eta / \sqrt{\bar{\phi}} \cdot \text{Gr}_z^{1/5} y/x$ ,  $\eta_1 = \eta_0/\gamma$  and  $\gamma = \sqrt{(1-1/\xi)\bar{\psi}/\bar{\phi}}$ . The values of  $\bar{C}_u$ ,  $\bar{C}_\eta$ ,  $\bar{\phi}$  and  $\bar{\psi}$  can be obtained from the appendix. The solutions to a problem in which the entire wall is maintained at  $q_{w0}$  can be found from Eqs. (18) and (19) by discarding the last terms and setting  $\bar{\phi} = 1$ . It is also reassuring to note that, in the limit, as the value of the Prandtl number approaches unity, all the expressions contained herein for  $\text{Pr} \neq 1$  become identical to those for  $\text{Pr} = 1$ .

Equations (18) and (19) are evaluated for a wide range of Prandtl numbers with various surface heat flux ratios,  $q_{w1}^*$ . The surface heat flux ratio for general values of  $\bar{a}$  is

$$q_{w1}^* = \frac{q_{w1}}{q_{w0}} = 1 + \frac{\beta}{A} \left( 1 - \frac{1}{\xi} \right)^{\bar{a}} \quad (22)$$

Dimensionless temperature and velocity distributions for  $x \leq x_0$  are shown in Figs. 1 and 2, respectively, for cases of uniform surface heat flux with the variables converted to those used in the study of Sparrow and Gregg (1956). These figures show good agreement between the results obtained by using the present method and those obtained by using the similarity methods. Figures 3 and 4 depict the dimensionless temperature and velocity field developments in air responding to a step change in uniform surface heat flux with  $q_{w1}^* = 1 + \beta/A = 0$

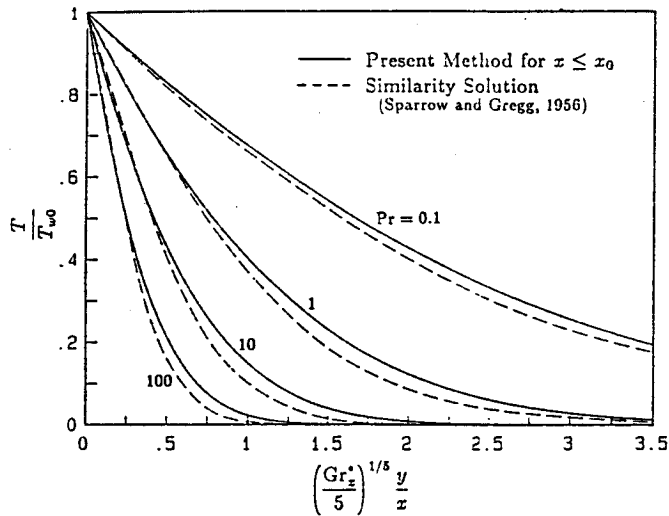


FIG. 1 COMPARISON OF DIMENSIONLESS TEMPERATURE DISTRIBUTIONS FOR VARIOUS PRANDTL NUMBERS WITH A UNIFORM SURFACE HEAT FLUX.

and 2, where  $T_{w0}$  is the wall temperature that would have been attained at the location of interest if the entire wall had been maintained at  $q_{w0}$ . Shown in Fig. 5 is the temperature distribution for the same parameters used in Fig. 3, except the value of  $\tilde{a}$  which is equal to  $-1/4$ . Figure 5 reveals the positive temperature gradient at the downstream locations near the wall, clearly depicting the heat transfer from the fluid to the plate when  $1 + \beta/A = 0$ . When  $\beta/A$  is less than zero,  $q_{w1}^*$  given by Eq. (22) is negative in the downstream region between  $\xi = 1$  and  $\xi = 1/[1 - (\beta/A)^4]$ .

The local wall temperature at the location  $x \leq x_0$  may be obtained from the first term of Eq. (18). Upon substituting  $\phi = 1$  and  $\eta_0 = 0$ , it yields

$$T_{w0} = \frac{1}{C_\eta} \frac{\Lambda(\tilde{n})}{\Lambda(\tilde{n}+1)} \frac{q_{w0}x}{kGr_x^{*1/5}} \quad (23)$$

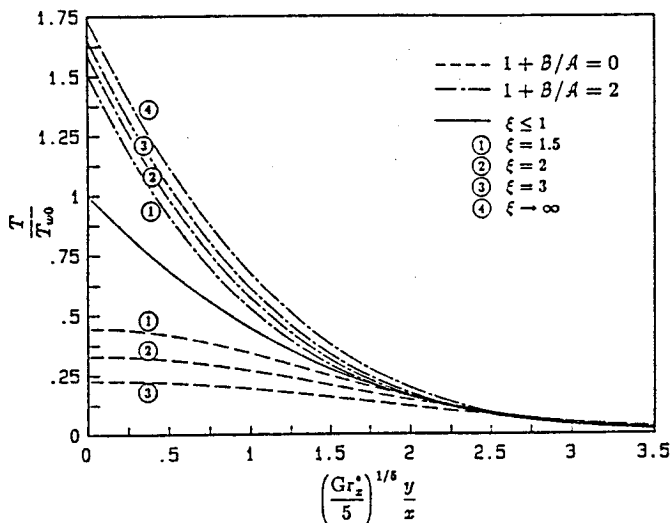


FIG. 3 DIMENSIONLESS TEMPERATURE FIELD DEVELOPMENT WITH A STEP CHANGE IN UNIFORM SURFACE HEAT FLUX,  $\tilde{a} = \tilde{b} = 0$ ;  $Pr = 0.7$ .

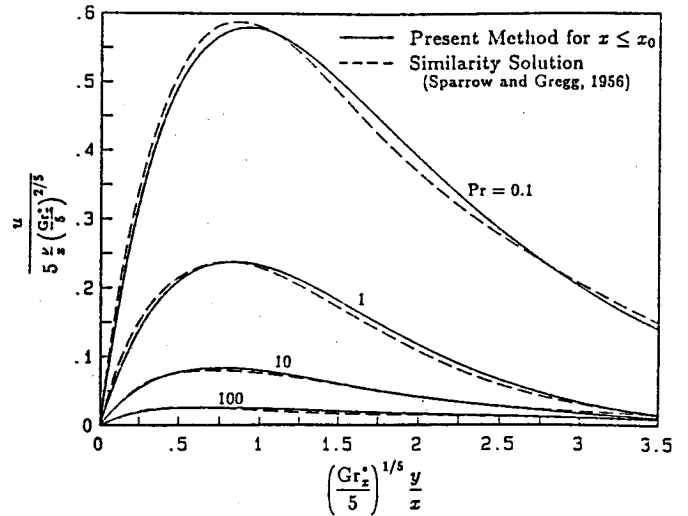


FIG. 2 COMPARISON OF DIMENSIONLESS VELOCITY DISTRIBUTIONS FOR VARIOUS PRANDTL NUMBERS WITH A UNIFORM SURFACE HEAT FLUX.

A dimensionless local heat transfer coefficient at  $x \leq x_0$  is, therefore,

$$\frac{Nu_x}{Ra_x^{*1/5}} = \frac{\tilde{C}_\eta}{Pr^{1/5}} \frac{\Lambda(\tilde{n}+1)}{\Lambda(\tilde{n})} \quad (24)$$

The coefficient is evaluated for the uniform surface heat flux case over a wide range of Prandtl numbers. For this case,  $\tilde{n} = 0$  results in  $\Lambda(\tilde{n}) = 1$  and  $\Lambda(\tilde{n}+1) = \sqrt{\pi}$ . This is compared to an existing correlation equation of Fujii and Fujii (1976) in Fig. 6, where a maximum difference of 17% is observed when the value of the Prandtl number is around  $10^6$ . The correlation equation is rewritten here as

$$\frac{Nu_x}{Ra_x^{*1/5}} = \left( \frac{Pr}{4 + 9\sqrt{Pr} + 10Pr} \right)^{1/5} \quad (25)$$

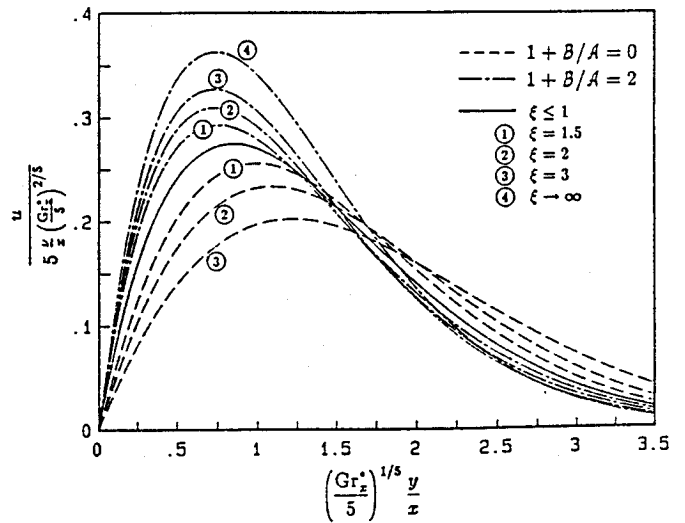


FIG. 4 DIMENSIONLESS VELOCITY FIELD DEVELOPMENT WITH A STEP CHANGE IN UNIFORM SURFACE HEAT FLUX,  $\tilde{a} = \tilde{b} = 0$ ;  $Pr = 0.7$ .

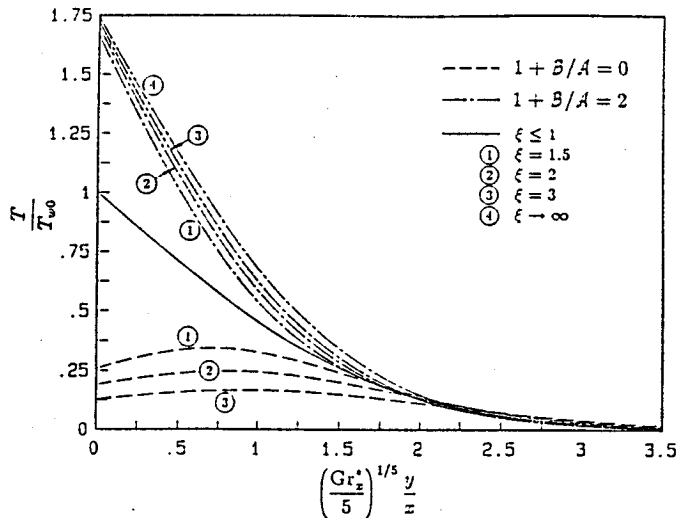


FIG. 5 DIMENSIONLESS TEMPERATURE FIELD DEVELOPMENT :  $\bar{a} = \bar{b} = -1/4$ ,  $Pr = 0.7$ .

A dimensionless local wall temperature at the location  $x > x_0$  may be expressed as

$$T_{w1}^* = \frac{T_{w1}}{T_{w0}} = \sqrt{\phi} [1 + (q_{w1}^* - 1)\gamma] \quad (26)$$

Notice that while the value of  $T_{w0}$  at fixed  $x$  differs depending on the expression chosen between the calculated and correlated coefficients,  $T_{w1}^*$ , given by Eq. (26), is independent of the choice.

The selected wall temperature variations obtained by using Eq. (26) are plotted in Figs. 7 and 8 for  $\bar{a} = 0$  and  $\bar{a} = -1/4$ , respectively. The values indicated by arrows are the asymptotic values at large  $x$ , and they are from

$$\lim_{z \rightarrow \infty} T_{w1}^* = \left(1 + \frac{B}{A}\right)^{4/5} \quad (27)$$

Both Figs. 7 and 8 depict the faster thermal response of a higher Prandtl number fluid to the surface heat flux change. Further, the responses seen from Fig. 8 are much faster when

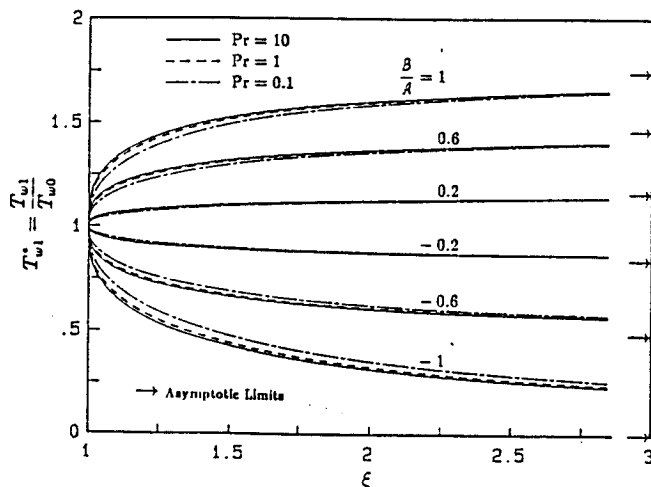


FIG. 7 WALL TEMPERATURE VARIATION :  $\bar{a} = \bar{b} = 0$ .

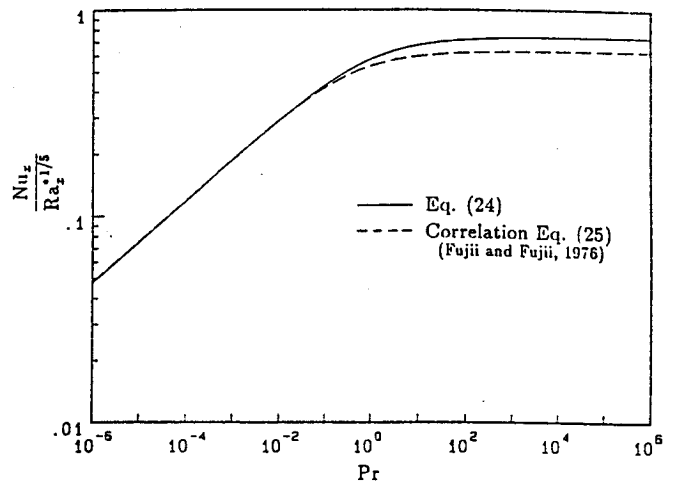


FIG. 6 COMPARISON OF  $Nu_x/Ra_x^{1/5}$  AS A FUNCTION OF PRANDTL NUMBER : UNIFORM SURFACE HEAT FLUX CASE.

compared with those seen from Fig. 7. From Eq. (23),  $T_{w0}$  is uniform when  $q_{w0}$  is proportional to  $x^{-1/4}$ . Since  $q_{w1} - q_{w0}$  is proportional to  $(x - x_0)^{-1/4}$  for  $x > x_0$ , the downstream wall temperature variations shown in Fig. 8 would be uniform and equal to the corresponding asymptotic values if superposition were valid in the  $x - y$  plane. Thus, the deviation of the wall temperature at  $x > x_0$  from their corresponding asymptotic values in Fig. 8 is attributed to the non-linear effects on the temperature field.

The wall temperature variation due to a finite size strip source of uniform surface heat flux, located on an adiabatic surface in air, is evaluated along the flow direction. The results are compared in Fig. 9 with Jaluria's numerical data (1985). Also compared in this figure is the local maximum streamwise velocity of the flow with the variables converted to those of Jaluria's study. Figure 9 contains an additional comparison between the results obtained by using the present method and those obtained by using the similarity methods (Jaluria and Gebhart, 1977), for a vertical adiabatic surface with a line

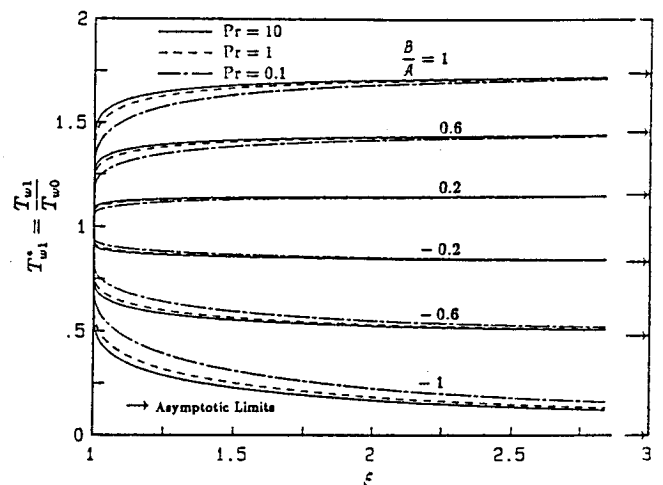


FIG. 8 WALL TEMPERATURE VARIATION :  $\bar{a} = \bar{b} = -1/4$ .

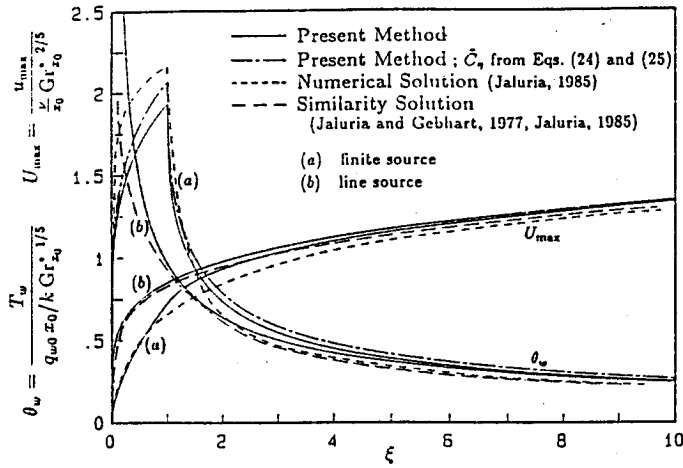


FIG. 9 COMPARISON OF WALL TEMPERATURE AND MAXIMUM VELOCITY VARIATIONS :  $q_{w1}^* = 0$ ,  $Pr = 0.7$ .

source located at the leading edge. The total amount of energy dissipated by the line source is sized to be the same as that dissipated by the strip source, so that the asymptotic behavior of the results may be examined. The present method simulates this line source by using a thin source, that has a width of one-hundredth of the strip source at the leading edge. Jaluria's results compared in Fig. 9 are retrieved by carefully discretizing his reported plots that are contained in the numerical study (Jaluria, 1985).

The comparisons are in good agreement. The qualitative behavior predicted by using the present method is essentially the same as that obtained by using the other methods. Unlike  $T_{w1}^*$  of Eq. (26), the magnitude of the dimensionless wall temperature,  $\theta_w$ , in Fig. 9 is dependent on the choice of the expression for the heat transfer coefficient. The values of  $\tilde{C}_u$  and  $\tilde{C}_\eta$  from the appendix are used in Eqs. (18) and (19) for the variations drawn by the solid lines. The wall temperature variation depicted by the chain line is also obtained from Eq. (18), except it is evaluated by using  $\tilde{C}_\eta$  that is directly obtained by equating Eqs. (24) and (25). It is worthwhile stressing that the difference in the values of  $\tilde{C}_\eta$  from these two different sources is a constant scaling factor, so that it alters the overall magnitude of the wall temperature variation while maintaining the surface heat flux as prescribed. Although the value of  $\tilde{C}_\eta$  obtained by equating Eqs. (24) and (25) conserves neither energy nor momentum over the boundary layer in general, it is recommended to be used when the Prandtl number is greater than 0.1, as the deviation in the heat transfer rate from that of the correlation equation of Fujii and Fujii (1976) becomes significant, as shown in Fig. 6. Jaluria's numerical prediction overestimates the wall temperature by approximately 5% at  $\xi = 1$ , when it is compared to the result of Eq. (18) evaluated with  $\tilde{C}_\eta$  from Eqs. (24) and (25).

The solutions, obtained by using the similarity methods for the case of uniform surface heat flux, indicate that the local wall temperature variation is proportional to  $x^{1/5}$ , and the maximum flow velocity is proportional to  $x^{3/5}$  (Sparrow and Gregg, 1956). The results reported by Jaluria and Gebhart (1977), who also used similarity methods for the case with a line source, show that the local wall temperature variation

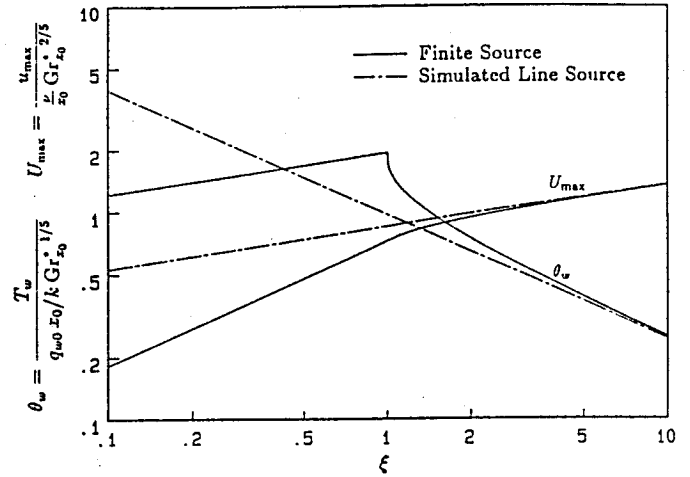


FIG. 10 WALL TEMPERATURE AND MAXIMUM VELOCITY VARIATIONS :  $q_{w1}^* = 0$ ,  $Pr = 0.7$ .

is proportional to  $x^{-3/5}$ , and the maximum flow velocity is proportional to  $x^{1/5}$ . Figure 10 reveals perfect agreement of the results obtained by using the present method in this regard.

The remainder of this section establishes relationships between the approximate solutions to problems with prescribed wall temperature variations of the power form and those with the prescribed surface heat flux variations for  $x \leq x_0$ .

Consider the governing differential equations, Eqs. (1-3), with the boundary conditions given by Eq. (4), except the thermal conditions at  $y = 0$  are replaced by

$$T = T_{w0} = Ax^a \quad (28)$$

where  $a$  and  $A$  are constants. The approximate solutions to this problem were found (Lee and Yovanovich, 1987) as

$$\frac{T}{T_{w0}} = \Lambda(n) i^n \text{erfc } \eta \quad (29)$$

$$\frac{u}{2\sqrt{g\beta T_{w0}x}} = \begin{cases} C_u \Lambda(n) \eta i^{n+1} \text{erfc } \eta & \text{for } Pr = 1 \\ C_u \Lambda(n) \frac{2}{1-Pr} (i^{n+2} \text{erfc } \eta - i^{n+2} \text{erfc } \frac{\eta}{\sqrt{Pr}}) & \text{for } Pr \neq 1 \end{cases} \quad (30)$$

where  $\eta = C_\eta (Gr_x/4)^{1/4} y/x$ ,  $\Lambda(\cdot)$  is as defined,  $Gr_x$  is the local Grashof number, and

$$n = \frac{4a}{1-a} \quad (31)$$

The coefficients  $C_u$  and  $C_\eta$  are constants that are analogous to  $\tilde{C}_u$  and  $\tilde{C}_\eta$ .

The above solutions become identical to Eqs. (18) and (19) for  $x \leq x_0$  when Eq. (23) is substituted for  $T_{w0}$  and the following relationships are satisfied:

$$C_\eta^4 = 4\tilde{C}_\eta^5 \frac{\Lambda(n)}{\Lambda(\tilde{n})} \quad (32)$$

$$C_u = \tilde{C}_u \left[ \frac{\tilde{C}_\eta \Lambda(\tilde{n})}{4 \Lambda(n)} \right]^{1/2} \quad (33)$$

$$n = \tilde{n} + 1 \quad (34)$$

The relationship between  $a$  and  $\bar{a}$  may be obtained from Eq. (34) by substituting Eqs. (13) and (31) for  $\bar{n}$  and  $n$ , respectively. That is

$$a = \frac{4\bar{a} + 1}{5} \quad (35)$$

The same relationship may be obtained by substituting  $T_{w0} = Ax^3$  and  $q_{w0} = Ax^3$  into Eq. (23). Equation (35) determines the functional variation of one type of boundary condition subjected to the other. Sparrow and Gregg (1958) have found this relationship by using similarity methods. The foregoing discussion indicates that a problem with a prescribed wall temperature variation and one with a prescribed surface heat flux variation are essentially the same problem when the variations are given in the power form.

#### ACKNOWLEDGEMENTS

The authors wish to acknowledge the financial support of the Natural Sciences and Engineering Research Council of Canada under a Postgraduate Scholarship for Mr. Lee, and operating grant A7455 for Dr. Yovanovich.

#### REFERENCES

- Abramowitz, M., and Stegun, I.A., 1965, *Handbook of Mathematical Functions*, Dover Publications, New York.
- Fujii, T., and Fujii, M., 1976, "The Dependence of Local Nusselt Number on Prandtl Number In the Case of Free Convection Along a Vertical Surface With Uniform Heat Flux," *Int. J. Heat Mass Transfer*, Vol. 19, pp. 121-122.
- Hayday, A.A., Bowls, D.A., and McGraw, R.A., 1967, "Free Convection From a Vertical Flat Plate With Step Discontinuities in Surface Temperature," *Trans. ASME*, series C., Vol. 89, No. 3, pp. 244-250.
- Jaluria, Y., and Gebhart, B., 1977, "Buoyancy-Induced Flow Arising From a Line Thermal Source on an Adiabatic Vertical Surface," *Int. J. Heat Mass Transfer*, Vol. 20, pp. 153-157.
- Jaluria, Y., 1982, "Buoyancy-Induced Flow Due to Isolated Thermal Sources on a Vertical Surface," *J. Heat Transfer*, Vol. 104, pp. 223-227.
- Jaluria, Y., 1985, "Interaction of Natural Convection Wakes Arising From Thermal Sources on a Vertical Surface," *J. Heat Transfer*, Vol. 107, pp. 883-892.
- Kao, T.T., 1975, "Laminar Free Convective Heat Transfer Response Along a Vertical Flat Plate With Step Jump in Surface Temperature," *Lett. Heat Mass Transfer*, Vol. 2, No. 5, pp. 419-428.
- Kelleher, M., 1971, "Free Convection From a Vertical Plate With Discontinuous Wall Temperature," *Trans. ASME*, Vol. 93, pp. 349-356.
- Kishinami, K., and Seki, N., 1983, "Natural Convective Heat Transfer on an Unheated Vertical Plate Attached to an Upstream Isothermal Plate," *J. Heat Transfer*, Vol. 105, pp. 759-766.
- Kishinami, K., Saito, H., and Tokura, I., 1987, "Natural Convective Heat Transfer on a Vertical Plate With Discontinuous Surface-Heating (Effect of Heat Conduction in Unheated Elements)," *Proc. of ASME-JSME Thermal Engineering Joint Conf.*, Vol. 4, pp. 61-68.
- Lee, S., 1988, PhD Thesis in progress, Dept. of Mechanical Engineering, University of Waterloo.
- Lee, S., and Yovanovich, M.M., 1987, "Laminar Natural Convection From a Vertical Plate With Variations in Wall Temperature," *ASME HTD-Vol. 82, Convective Transport*, ed. Y. Jaluria, R.S. Figliola and M. Kaviany, ASME Winter Annual Meeting, December 13-18, 1987, Boston, MA.
- Menold E.R., and Yang K.T., 1962, "Asymptotic Solutions for Unsteady Laminar Free Convection on a Vertical Plate," *J. Appl. Mech.*, Vol. 29, *Trans. ASME*, Vol. 84, pp. 124-126.
- Schetz, J.A., and Eichhorn, R., 1962, "Unsteady Natural Convection in the Vicinity of a Doubly Infinite Vertical Plate," *Trans. ASME*, Vol. 84, pp. 334-338.
- Schetz, J.A., and Eichhorn, R., 1964, "Natural Convection With Discontinuous Wall-Temperature Variations," *J. Fluid Mech.*, Vol. 18, part 2, pp. 167-176.
- Smith, R.K., 1970, "The Laminar Free-Convection Boundary Layer on a Vertical Heated Plate in the Neighbourhood of a Discontinuity in Plate Temperature," *J. Austral. Math. Soc.*, Vol. 11, No. 2, pp. 149-168.
- Sokovishin, Y.A., and Éрман, L.A., 1982, "Free-Convection Heat Transfer on a Vertical Surface With a Temperature Discontinuity," *J. Eng. Phys.*, Vol. 43, No. 2, pp. 858-861.
- Sparrow, E.M., and Gregg, J.L., 1956, "Laminar Free Convection From a Vertical Plate With Uniform Surface Heat Flux," *Trans. ASME*, Vol. 78, pp. 435-440.
- Sparrow, E.M., and Gregg, J.L., 1958, "Similar Solutions for Free Convection From a Nonisothermal Vertical Plate," *Trans. ASME*, Vol. 80, pp. 379-386.
- Zinnes, A.E., 1970, "The Coupling of Conduction With Laminar Natural Convection From a Vertical Flat Plate With Arbitrary Surface Heating," *J. Heat Transfer*, Vol. 92, pp. 528-535.

#### APPENDIX

Derivation of  $\bar{C}_u$  and  $\bar{C}_\eta$ . The dimensionless proportionality constants,  $\bar{C}_u$  and  $\bar{C}_\eta$ , needed in the  $t - x$  transformation functions for  $x \leq x_0$  may be evaluated by using the von Kármán-Pohlhausen integral method. Integration of the momentum and energy equations, Eqs. (2) and (3), across the boundary layer, followed by another integration of the energy equation from the leading edge of the plate,  $x = 0$ , to the location of interest yields

$$\frac{d}{dx} \int_0^\infty u^2 dy + \nu \left( \frac{\partial u}{\partial y} \right)_{y=0} = g\beta \int_0^\infty T dy \quad (A.1)$$

$$\frac{k}{\alpha} \int_0^\infty Tu dy = \int_0^x q_w dz \quad (A.2)$$



where we have used the continuity equation, Eq. (1). Although direct substitutions of the solutions given by Eqs. (18) and (19) for  $x \leq x_0$  into the above integral equations provide the identical results, it is simpler to utilize the forefound relationships given by Eqs. (32) and (33). They express  $\bar{C}_u$  and  $\bar{C}_\eta$  in terms of  $C_u$  and  $C_\eta$ , where  $C_u$  and  $C_\eta$  can be obtained from the appendix of the earlier study (Lee and Yovanovich, 1987) with corresponding values of  $n$  and  $a$  as defined by Eqs. (34) and (35).

**Derivation of  $\bar{\phi}$  and  $\bar{\psi}$ .** The modifying functions  $\bar{\phi}$  and  $\bar{\psi}$ , required in the  $t-x$  transformations for  $x > x_0$ , are evaluated by using the von Kármán-Pohlhausen integral method for the wall conditions prescribed in Eq. (4). For simplicity, however, only the conditions where  $\bar{a} = \bar{b}$  are concerned in this derivation. Substitute solutions given by Eqs. (18) and (19) for  $T$  and  $u$ , respectively, and Eq. (4) for  $q_w$  into Eqs. (A.1) and (A.2), evaluate, simplify, and rearrange to obtain

$$\frac{5}{3\bar{a} + 7} \frac{1}{\xi^{(3\bar{a}+7)/5}} \frac{d}{d\xi} \left[ \xi^{(3\bar{a}+7)/5} \bar{\phi}^{7/2} \mathcal{M}_m \right] = q_m^* \quad (\text{A.3})$$

$$\bar{\phi}^{5/2} \mathcal{M}_e = q_e^* \quad (\text{A.4})$$

where

$$\mathcal{M}_m = 1 + (q_{w1}^* - 1)^2 \gamma^7 + (q_{w1}^* - 1) \gamma h_m \quad (\text{A.5})$$

$$\mathcal{M}_e = 1 + (q_{w1}^* - 1)^2 \gamma^5 + (q_{w1}^* - 1) \gamma h_e \quad (\text{A.6})$$

$$q_m^* = 1 + (q_{w1}^* - 1) \gamma^2 \quad (\text{A.7})$$

$$q_e^* = 1 + (q_{w1}^* - 1) \left(1 - \frac{1}{\xi}\right) \quad (\text{A.8})$$

and  $\xi = x/x_0$ ,  $\gamma = \sqrt{(1-1/\xi)} \bar{\psi}/\bar{\phi}$ . Here, the relationship between  $\bar{C}_u$  and  $\bar{C}_\eta$  was used, and

$$\gamma h_m = \gamma \frac{2\gamma^3 \int_0^\infty f_u(\gamma\eta) f_u(\eta) d\eta}{\int_0^\infty f_u^2(\eta) d\eta} \quad (\text{A.9})$$

$$\gamma h_e = \gamma \frac{\gamma^3 \int_0^\infty f_T(\gamma\eta) f_u(\eta) d\eta + \int_0^\infty f_T(\eta/\gamma) f_u(\eta) d\eta}{\int_0^\infty f_T(\eta) f_u(\eta) d\eta} \quad (\text{A.10})$$

where  $f_T(\cdot)$  and  $f_u(\cdot)$  are defined by Eqs. (20) and (21), respectively.

The parameters  $h_m$  and  $h_e$  are both functions of  $\bar{n}$ , Pr, and  $\gamma$ . Although it is possible to derive recurrence relationships for  $h_m$  and  $h_e$  in terms of  $\bar{n}$ , only the expressions for the case where  $\bar{n} = 0$ , a step change in uniform surface heat flux, are shown below for brevity. They are, for Pr = 1,

$$\gamma h_m = \frac{12\gamma^7 + 7\gamma^5 + 7\gamma^2 + 12 + 35\gamma^2(1+\gamma^2)^{3/2} - 12(1+\gamma^2)^{7/2}}{19 - 13\sqrt{2}} \quad (\text{A.11})$$

$$\gamma h_e = \frac{2\gamma^5 + 5\gamma^3 + 5\gamma^2 + 2 - 2(1+\gamma^2)^{5/2}}{7 - 4\sqrt{2}} \quad (\text{A.12})$$

or, for Pr  $\neq$  1,

$$\begin{aligned} \gamma h_m = & \left[ (1-p)(1-p^2) \{ 7p^2\gamma^2(1+\gamma^3) + 2(1+p^2)(1+p-p^2)(1+\gamma^7) \} \right. \\ & \left. + 2p^3(1+p)(1+\gamma^2)^{7/2} - 2(p^2+\gamma^2)^{7/2} - 2(1+p^2\gamma^2)^{7/2} \right] \\ & \div \left[ 2p^7 + 7p^5 + (8\sqrt{2}-9)(p^4+p^3) + 7p^2 + 2 - 2(1+p^2)^{7/2} \right] \end{aligned} \quad (\text{A.13})$$

$$\begin{aligned} \gamma h_e = & \left[ 4p^3(1+\gamma^2)^{5/2} - 2(1+p^2\gamma^2)^{5/2} - 2(p^2+\gamma^2)^{5/2} \right. \\ & \left. + 2(1-2p^2+p^5)(1+\gamma^5) + 5p^2\gamma^2(1-p)(1+\gamma) \right] \\ & \div \left[ 2p^5 + (8\sqrt{2}-9)p^3 + 5p^2 + 2 - 2(1+p^2)^{5/2} \right] \end{aligned} \quad (\text{A.14})$$

where  $p = \sqrt{\text{Pr}}$ .

The corresponding expressions for the case where  $\bar{n} = -1$  or  $\bar{a} = -1/4$  may also be found in the appendix of the earlier study that was carried out by Lee and Yovanovich (1987), for the case with a step change in uniform wall temperature.

Expanding the derivative, Eq. (A.3) becomes

$$\bar{\phi}^{5/2} \mathcal{M}_m + \frac{5\xi}{3\bar{a} + 7} \left[ \frac{7}{5} \frac{d\bar{\phi}^{5/2}}{d\xi} \mathcal{M}_m + \bar{\phi}^{5/2} \frac{d\mathcal{M}_m}{d\xi} \right] = q_m^* \quad (\text{A.15})$$

Under a further manipulation, this becomes

$$\frac{d\gamma^3}{d\xi} = \frac{\frac{1}{35\xi^2} \left[ (3\bar{a}+7) \left( q_m^* \frac{\mathcal{M}_e}{\mathcal{M}_m} - q_{w1}^* \right) - \frac{4\bar{a}}{\xi} (q_{w1}^* - 1) \right] - \frac{\partial \mathcal{M}_m}{\partial \xi} + \frac{\partial \mathcal{M}_e}{\partial \xi}}{\frac{\partial \mathcal{M}_m / (7\gamma^2 \partial \gamma)}{3\mathcal{M}_m} - \frac{\partial \mathcal{M}_e / (5\gamma^2 \partial \gamma)}{3\mathcal{M}_e}} \quad (\text{A.16})$$

and  $\gamma^3 = 0$  at  $\xi = 1$ .

This initial value of  $\gamma^3$  at  $\xi = 1$  can be obtained by considering the conditions that have to be satisfied at  $\xi = 1$ . It is clear that at  $\xi = 1$ , or  $x = x_0$ , the  $t-x$  transformations for  $x \leq x_0$  and those for  $x > x_0$  should be continuous, resulting in  $\bar{\phi} = 1$ . Hence Eq. (A.4) results in  $\mathcal{M}_e = 1$ , and in turn, Eq. (A.6) suggests  $\gamma = 0$ .

Equation (A.4) and the following expressions were used in the above manipulation.

$$\frac{d\bar{\phi}^{5/2}}{d\xi} = \frac{1}{\mathcal{M}_e} \left[ \frac{\bar{a}+1}{\xi^2} (q_{w1}^* - 1) - \bar{\phi}^{5/2} \frac{d\mathcal{M}_e}{d\xi} \right] \quad (\text{A.17})$$

$$\frac{d\mathcal{M}}{d\xi} = \frac{\partial \mathcal{M}}{\partial \xi} + \frac{\partial \mathcal{M}}{3\gamma^2 \partial \gamma} \frac{d\gamma^3}{d\xi} \quad (\text{A.18})$$

where, Eq. (A.17) is derived from Eq. (A.4), and  $\mathcal{M}$  denotes either  $\mathcal{M}_m$  or  $\mathcal{M}_e$ . Equation (A.18) is formed such that singularity problems anticipated in the numerical evaluation of Eq. (A.16) are avoided. Also, the partial derivatives of  $\mathcal{M}_m$  and  $\mathcal{M}_e$  with respect to  $\xi$  and  $\gamma$  may be obtained from Eqs. (A.5) and (A.6).

Equation (A.16) combined with Eqs. (A.5) through (A.10) is a first order ordinary differential equation that may be solved numerically for  $\gamma^3$  with given  $q_{w1}^*$  and Pr. Note that this differential equation becomes considerably simpler when  $\bar{a} = 0$ , the case of a step change in uniform surface heat flux, since the last three terms in the numerator vanish. Upon finding  $\gamma^3$ ,  $\bar{\phi}$  and  $\bar{\psi}$  can be obtained respectively from Eq. (A.4) and the definition of  $\gamma$  stated earlier.